Bound Pulse Trains in Arrays of Coupled Spatially Extended Dynamical Systems

D. Puzyrev,[1] A. G. Vladimirov,[2,3] A. Pimenov,[2] S. V. Gurevich,[4,5] and S. Yanchuk[1]
[1]Institute of Mathematics, Technische Universität Berlin, Strasse des 17. Juni 136, D-10623 Berlin, Germany
[2]Weierstrass Institute for Applied Analysis and Stochastics, Mohrenstrasse 39, D-10117 Berlin, Germany
[3]Lobachevsky State University of Nizhni Novgorod, pr.Gagarina 23, Nizhni Novgorod 603950, Russia
[4]Institute for Theoretical Physics, University of Münster, Wilhelm-Klemm-Strasse 9, D-48149 Münster, Germany
[5]Center for Nonlinear Science (CeNoS), University of Münster, Corrensstrasse 2, D-48149 Münster, Germany
(Received 5 April 2017; revised manuscript received 14 September 2017; published 19 October 2017)

We study the dynamics of an array of nearest-neighbor coupled spatially distributed systems each generating a periodic sequence of short pulses. We demonstrate that, unlike a solitary system generating a train of equidistant pulses, an array of such systems can produce a sequence of clusters of closely packed pulses, with the distance between individual pulses depending on the coupling phase. This regime associated with the formation of locally coupled pulse trains bounded due to a balance of attraction and repulsion between them is different from the pulse bound states reported earlier in different laser, plasma, chemical, and biological systems. We propose a simplified analytical description of the observed phenomenon, which is in good agreement with the results of direct numerical simulations of a model system describing an array of coupled mode-locked lasers.

DOI: 10.1103/PhysRevLett.119.163901

Nonlinear temporal pulses and spatial dissipative localized structures appear in various optical, plasma, hydrodynamic, chemical, and biological systems [1–13]. Being well separated from each other in time or space, these structures can interact locally via exponentially decaying tails. As a result of this interaction, they can form bound states, known also as "dissipative soliton molecules" [5,10,11,14], characterized by fixed distances and phase differences between individual pulses. Such bound states can emerge due to the oscillatory character of the interaction force which is related to the presence of oscillating tails. Another scenario occurs in the case of monotonic repulsive interaction when either the pulse tails decay monotonically or a strong nonlocal repulsive interaction between the pulses is present. In this case, the pulses tend to distribute equidistantly in time or space, leading to periodic pulse trains [15–18], which, in contrast to closely packed bound states, exhibit large distances between the consequent pulses. Recently, it was shown that pointwise nonlocality may also lead to the formation of molecules composed by pulses which are globally bounded but locally independent [19].

In this Letter, we show that, even in the case when the pulses in an individual system exhibit strong repulsion, the formation of bound pulse trains can be achieved by arranging several systems in an array with nearest-neighbor coupling. As a result, the pulses interact not only within one system but also with those in the neighboring ones, leading to a different balance of attraction and repulsion. More specifically, we demonstrate that this array can produce a periodic train of clusters consisting of two or more closely packed pulses with the possibility to change the interval between them via the variation of the coupling phase parameter. Such bound pulse trains cannot exist in a solitary pulse-generating systems and hence are different from pulse bound states previously observed in, e.g., Refs. [14,20–33].

To clarify the origin of this phenomenon for the case of two coupled systems, we apply a multiscale method to derive a reduced system of equations governing the slow time evolution of the phase difference and distance between the two interacting pulse trains. Furthermore, we demonstrate that the observed pulse train states can coexist with the in- and antiphase synchronized regimes in which all pulses have identical amplitudes and the phases of the adjacent pulses are either in or antiphase. Note that, in contrast to the pulse bound state regime, such types of in- and antiphase synchronization are well known in coupled oscillator networks [34,35]. To illustrate our general result, we focus on a particular example of an array of mode-locked lasers coupled via evanescent fields in a ring geometry; see Fig. 1(a). Such lasers are widely used for the generation of short optical pulses with high repetition rates and optical frequency combs suitable for numerous applications [37]. Combining many lasers into an array, one can achieve a much larger output power and substantially improve the characteristics of the output beam by synchronizing the frequencies of the individual lasers [38].

We assume that each individual array element generates a periodic pulse train, and it is described by a system of delay differential equations (DDEs). Then the dynamics of an array of N such elements is given by the set of symmetrically coupled systems of nonlinear DDEs:

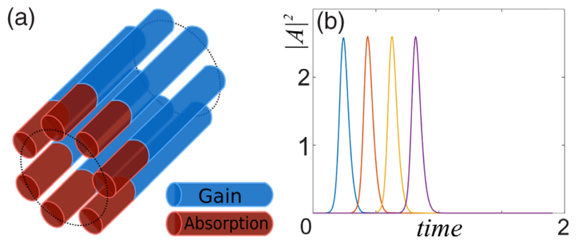

FIG. 1. (a) Schematic representation of a ring array of nearest-neighbor coupled mode-locked lasers. (b) Laser intensities in the bound pulse train regime in a ring of four lasers calculated for $\eta = 0.5$ and $\varphi = 3.0$. Different colors correspond to different lasers. Other parameters: $\gamma = 33.3$, $\kappa = 0.1$, $\alpha_g = 2.0$, $\alpha_q = 3.0$, $\vartheta = 0$, $G_0 = 2.0$, $Q_0 = 4.0$, $\gamma_g = 0.0133$, $\gamma_q = 1$, $s = 25$, and $\tau = 1.875$ (similarly to Ref. [36]).

$$\frac{d\mathbf{u}_j}{dt} = \mathbf{F}[\mathbf{u}_j(t), \mathbf{u}_j(t-\tau)] + C(\mathbf{u}_{j-1} + \mathbf{u}_{j+1}), \qquad (1)$$

where $\mathbf{u}_j$, $j = 1, \ldots, N$, is the state variable describing the jth system and C is the coupling matrix. We assume that in the absence of coupling, $C = 0$, the system (1) generates periodic pulses with the period close to the delay time τ. Here we consider a particular model for a passively mode-locked laser [36] for the array elements. In this case, $\mathbf{u} = (A(t), G(t), Q(t))^T$, where A denotes the complex electric field amplitude whereas G and Q are saturable gain and loss, respectively. The components of the function $\mathbf{F}$ are $F_1 = -\gamma A + \gamma\sqrt{\kappa} R A(t-\tau)$, $F_2 = G_0 - \gamma_g G - e^{-Q}(e^G - 1)|A(t-\tau)|^2$, and $F_3 = Q_0 - \gamma_q Q - s(1-e^{-Q})|A(t-\tau)|^2$, with $R = \exp[(1-i\alpha_g)G - (1-i\alpha_q)Q]/2 - i\vartheta$. The parameter γ represents the spectral filtering bandwidth, κ is the attenuation factor describing linear nonresonant intensity losses per cavity round trip, G_0 is the pump parameter, which is proportional to the injection current in the gain region, Q_0 is the unsaturated absorption parameter, γ_g and γ_q are the carrier relaxation rates in the amplifying and absorbing sections, and s is the ratio of the saturation intensities in these two sections. In what follows, we limit our analysis to the physically meaningful situation when the lasers are coupled via evanescent fields and, hence, the coupling matrix C has only a single nonzero element $C_{11} = \eta e^{i\varphi}$, where η is the coupling strength and φ is the coupling phase. Note that the choice of a set of DDEs as a model system is particularly motivated by the fact that DDE models are proven to be very good test-bed systems for revealing various phenomena in spatially extended systems [39–41].

In the absence of coupling, $\eta = 0$, for the chosen parameter values each laser operates in a stable fundamental passive mode-locking regime with a single sharp pulse per cavity round trip time [36]. This regime can be represented in the form with $A_j(t) = \mathcal{A}(t+\theta_j)e^{i\omega t + i\phi_j}$, $G_j = \mathcal{G}(t+\theta_j)$, and $Q_j = \mathcal{Q}(t+\theta_j)$, where $\mathcal{A}(t)$, $\mathcal{G}(t)$, and $\mathcal{Q}(t)$ are periodic in time with the period T close to the delay τ, and arbitrary constant phase shifts θ_j and ϕ_j. For small coupling η, the time shifts θ_j and the phase shifts ϕ_j start evolving slowly in time due to the interaction between the lasers, and, as a result, a synchronized state can be achieved. In particular, due to the index shift symmetry of the system, solutions with identical amplitudes $|A_j(t)| = |A(t)|$ and a constant phase shift between the adjacent lasers $\upsilon_{j+1} - \upsilon_j = 2\pi l/N$, $l = 0, \ldots, N-1$ [42–47], are observed. The simplest types of the synchronized regimes are complete in-phase synchronization ($l = 0$) and antiphase synchronization ($l = N/2$ for an even number of lasers N). Note that there is also a potentially interesting "noninvasive" case $l = N/4$, for which the coupling vanishes: $A_{j-1} + A_{j+1} = 0$. For odd values of N, however, the antiphase and noninvasive synchronization regimes do not exist.

Stability regions for the in-phase and antiphase synchronized mode-locked solutions of the system of four lasers obtained using the master stability function approach [48] in the (φ, η) plane of coupling parameters are shown in Fig. 2(a). The form of the coupling implies that these stability regions are shifted relative to each other by π with respect to the coupling phase angle φ.

Along with the synchronized solutions, a new *bound pulse train regime* is observed for the parameter values shown in Fig. 2(b). In this regime, lasers pulse sequentially on the ring one after another, as shown in Fig. 1(b), while each of the lasers stays close to its fundamental mode-locked regime with a period τ_0 close to the delay time τ. The bound pulse train regime emerges from the synchronized solution at the supercritical pitchfork bifurcation [see line P in Fig. 2(b)]. The observed regime can be

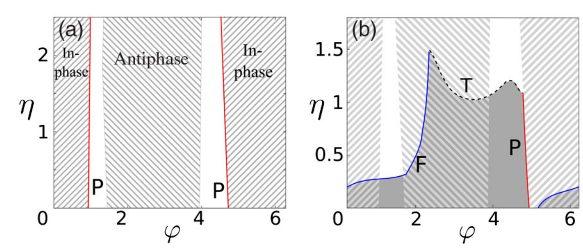

FIG. 2. (a) Bifurcation diagram in coordinates (φ, η) for the synchronized solutions in the ring array with $N = 4$. Left- and right-inclined hatching indicates the stability regions for the in-phase ($l = 0$) and antiphase ($l = 2$) synchronized solutions. Red lines P correspond to pitchfork bifurcations of the in-phase synchronized solution. (b) Bifurcation diagram for the bound state **B1** (cf. Fig. 4) in the plane (φ, η). The same as in panel (a), in addition, the light gray area shows the stability domain of the bound state. The red line P corresponds to a supercritical pitchfork bifurcation of the in-phase synchronized solution leading to the bound pulse train regime, the blue line F corresponds to a fold bifurcation where stable and unstable branches of bound pulse train solutions merge and disappear, and the dashed black line T shows the first torus bifurcation of the pulse bound state which leads to a modulation in a form of slight change of the pulse shapes from one pulse period to another.

better visualized using the so-called pseudospatial coordinates plane (T, σ) [41], where $\sigma = t \bmod \tau_0$ is the original fast time and $T = t/\tau_0$ is the slow time (number of round trips, $\tau_0 = \tau + 0.03$); see Fig. 3(a). We observe that pulses that were initially distributed on the interval $\sigma \in [0, \tau_0]$ start to interact and finally form a bound cluster. The distance between the pulses in this cluster can be controlled by changing the coupling phase φ, which determines the relative phase of the interacting pulse tails.

A similar bound pulse train for the case of two coupled lasers is shown in Fig. 3(b). In what follows, we investigate the origin of this bound state by applying the multiscale method [49–51] to the two-laser system in order to find the reduced system governing the slow dynamics of the time separation between the pulses and their phase differences. The generalization of this approach to the case of N coupled lasers is discussed in Supplemental Material [52].

To apply the multiscale method to Eq. (1), we consider the limit of small coupling, $\eta = \varepsilon\mu$ with a small parameter ε, and search for the solution of system (1) in the form $A_j(t_0,t_1) = \{e^{i\phi_j(t_1)}\mathcal{A}[t_0+\theta_j(t_1)] + \varepsilon A_j^1(t_0,t_1)\}e^{i\omega t_0}$, $G_j = \mathcal{G}[t_0+\theta_j(t_1)] + \varepsilon G_j^1(t_0,t_1)$, $Q_j = \mathcal{Q}[t_0+\theta_j(t_1)] + \varepsilon Q_j^1(t_0,t_1)$. Here $\mathcal{A}$, $\mathcal{G}$, and $\mathcal{Q}$ are a τ_0-periodic solution of the unperturbed system (mode-locked regime in an uncoupled laser), A_j^1, G_j^1, and Q_j^1 describe first-order corrections due to the coupling, and $t_0 = t$ and $t_1 = \varepsilon t$ are fast and slow times, respectively.

In the following, we explain how the reduced system (7) for the time separation $\Theta = \theta_2 - \theta_1$ between the pulses and the phase difference $\Phi = \phi_2 - \phi_1$ between pulse peaks can be obtained. For this purpose, the ansatz above is substituted into (1), and the resulting system is expanded in orders of ε (see [49–51] for details). Collecting the first-order terms in ε, we obtain the following linear system of DDEs for the perturbations $S_j = (\mathrm{Re}A_j^1, \mathrm{Im}A_j^1, G_j^1, Q_j^1)^T$:

$$\begin{aligned} &-\dot{S}_j + a_1(t)S_j(t) + a_2(t)S_j(t-\tau) \\ &\quad = a_3\dot{\theta}_j + a_4\dot{\phi}_j + \mathcal{R}[(-1)^j\Theta, (-1)^j\Phi], \quad j = 1, 2, \end{aligned} \tag{2}$$

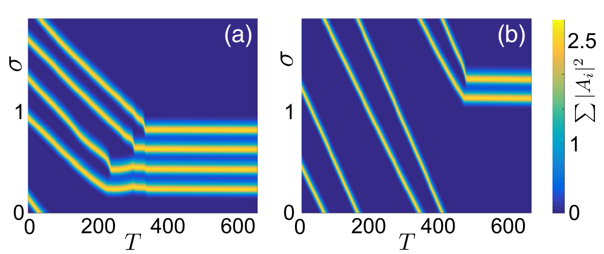

FIG. 3. (a) Space-time diagram of the bound pulse train regime in a four-laser array in coordinates (T, σ), where $\sigma = t \bmod \tau_0$ is the original fast time and $T = t/\tau_0$ the slow time ($\tau_0 = 1.9054$). Brighter colors indicate higher values of the sum of the laser intensities $\sum_{i=1}^4 |A_i|^2$. (b) Space-time diagram for the pulse train bound state regime for two lasers ($\tau_0 = 1.9043$). Coupling parameters are $\eta = 0.5$ and $\varphi = 3.0$.

with linear operators $a_{1,2}$ and vector functions $a_{3,4}$ depending only on the unperturbed pulse solution. Expressions for $a_{1,2,3,4}$ and $\mathcal{R}$ are given in Supplemental Material [52].

The solvability condition of the linear nonhomogeneous system (2) requires that its right-hand side is orthogonal to the neutral (or Goldstone) modes of the adjoint homogenous system [53]. In the case of a small coupling coefficient, $\eta \ll 1$, these modes can be approximated by a linear combination of the neutral modes of pulsed solutions of two uncoupled laser equations, $\psi_j^\dagger$ and $\xi_j^\dagger$ with $j = 1, 2$, related to the phase shift and the time-shift symmetries, respectively. These modes can be found numerically (see, e.g., [49–51]). The orthogonality of the right-hand side of (2) to $\psi_{1,2}^\dagger$ with respect to the inner product $\int_0^T \{a_3\dot{\theta}_j + a_4\dot{\phi}_j + \mathcal{R}[(-1)^j\Theta, (-1)^j\Phi]\}\psi_j^\dagger(t)dt = 0$ leads to the system of two ordinary differential equations

$$p_\psi\dot{\theta}_1 + q_\psi\dot{\phi}_1 = \mu R_\psi(\Theta, \Phi), \tag{3}$$

$$p_\psi\dot{\theta}_2 + q_\psi\dot{\phi}_2 = \mu R_\psi(-\Theta, -\Phi), \tag{4}$$

where coefficients p_ψ, q_ψ, and R_ψ are given by the corresponding inner products (cf. Supplemental Material [52]). Subtracting Eqs. (3) and (4) from one another, one obtains the equation for the phase difference Φ and time separation of the pulses Θ:

$$p_\psi\dot{\Theta} + q_\psi\dot{\Phi} = \mu[R_\psi(-\Theta, -\Phi) - R_\psi(\Theta, \Phi)]. \tag{5}$$

In the same way, the orthogonality conditions to the modes $\xi_{1,2}^\dagger$ lead to the equation

$$p_\xi\dot{\Theta} + q_\xi\dot{\Phi} = \mu[R_\xi(-\Theta, -\Phi) - R_\xi(\Theta, \Phi)]. \tag{6}$$

Solving now (5) and (6) for $\dot{\Theta}$ and $\dot{\Phi}$, we obtain the reduced system of two ordinary differential equations for the slow time evolution of Θ and Φ:

$$\begin{aligned} \dot{\Theta} &= \eta\cos[\Phi + \Delta_\Theta(\Theta)]f_\Theta(\Theta), \\ \dot{\Phi} &= \eta\sin[\Phi + \Delta_\Phi(\Theta)]f_\Phi(\Theta), \end{aligned} \tag{7}$$

where $f_{\Theta,\Phi}(\Theta) \geq 0$. The specific shape of the right-hand side of (7) is due to the fact that the function $R_\psi(\Theta, \Phi)$ contains only a first Fourier harmonic in Φ. As a result, the dependence on Φ is a linear combination of $\sin(\Phi)$ and $\cos(\Phi)$ that can be represented as (7). More details are given in Supplemental Material [52].

The bound pulse train states correspond to the fixed points of (7). These points are defined by the condition $\cos[\Phi + \Delta_\Theta(\Theta)] = \sin[\Phi + \Delta_\Phi(\Theta)] = 0$, which implies that one of the two conditions should be satisfied: $\Delta_\Theta(\Theta) = \Delta_\Phi(\Theta)$ or $\Delta_\Theta(\Theta) = \Delta_\Phi(\Theta) + \pi$. The first condition corresponds to the saddles of the system (7), while the second equation corresponds either to nodes or to foci. These equilibria correspond to pulse bound states of Eq. (1). Note that at zero pulse separation of the two pulses, $\Theta = 0$, the system (7) transforms into a single equation $\dot{\Phi} = \mu C_{\Phi} \sin\Phi$, which admits either in-phase $\Phi = 0$ or antiphase synchronization $\Phi = \pi$.

Noteworthily, the reduced system (7) resembles the equations governing the slow dynamics of the distance and phase difference between two interacting dissipative solitons in spatially extended systems described by the generalized complex Ginzburg-Landau equation on an unbounded domain [28,54–56]. The case of coupled lasers, however, is distinct in two aspects: (i) Unlike the case of the complex Ginzburg-Landau equation, the presence of the phase shifts $\Delta_{\Theta,\Phi}(\Theta)$ in Eq. (7) allows for the existence of bound states with the Θ-dependent phase difference between the pulses different from 0, π, and $\pm\pi/2$, and (ii) instead of a countable set of equidistant roots, the functions $f_{\Theta,\Phi}(\Theta)$ have no roots at all, which means that in laser arrays there is a finite number of bound states which are distributed along the Θ axis in a more complex manner.

The 2D phase plane of the reduced system (7) is presented in Fig. 4, where the equilibria and their basins of attraction are shown. Each single-colored region determines a set of pulse separations and phase differences, starting from which the system evolves to a single attractor (points **B1**–**B3** and **C1**) characterized by fixed Θ and Φ. Note that due to the symmetry $(\Theta, \Phi) \to (-\Theta, -\Phi)$ it is sufficient to consider the left half of the coordinate system. Here, the point **C1** corresponds to a stable antiphase synchronized solution, while points **B1**, **B2**, and **B3** indicate the bound states with nonzero pulse time separations Θ. Figure 4 shows the case of $\varphi = 3.0$. For other values of φ, there can coexist up to five stable equilibria corresponding to distinct bound states. Interestingly, the basin boundaries of these states can wind into unstable spiral sources as shown in the inset in Fig. 4. The video illustrating the position of the equilibria and corresponding basins of attraction for different values of φ is available in Supplemental Material [52].

A more detailed stability analysis of the bound state corresponding to the equilibrium **B1** is performed numerically using the path continuation software DDE-BIFTOOL [57] applied to Eq. (1). The bifurcation diagram showing the domain of stability and primary bifurcations of this bound state is presented in Fig. 2(b).

It is noteworthy that, due to the asymmetry of the single pulse shape, the time separations and phase shifts between adjacent pulses in the bound pulse train as well as their velocities depend on the number of lasers N. The solution of the reduced system in the case of N lasers (Sec. B in Supplemental Material [52]) as well as direct numerical simulations for $N = 4$ and $N = 7$ suggest that the formation of bound pulse trains with a large number of pulses can be qualitatively understood in terms of pairwise interaction between the adjacent pulses.

In conclusion, we discovered the bound pulse train regime in an array of nearest-neighbor coupled nonlinear distributed dynamical systems. In this regime, trains of short pulses generated by individual elements of the array are bound by local interaction, forming the closely packed pulse clusters. In the limit of small coupling strength, asymptotic equations are derived governing the slow time evolution positions and phases of the interacting pulses in an array consisting of two pulse generators. The pulse separations and phase differences between the pulses in bound states as well as basins of attraction of different bound states calculated using this semianalytical approach are in good agreement with the results of direct numerical simulations of a set of DDEs describing an array of coupled mode-locked lasers (1). The stability and bifurcations of bound pulse train regime were studied numerically with the path-following technique. The bound states reported in this Letter have a similarity with rather well-studied bound states of dissipative solitons in spatially extended systems, where multiple soliton clusters surrounded by a linearly stable homogeneous regime can be formed due to a similar mechanism of balancing between attraction and repulsion. However, unlike the bound states formed by dissipative solitons, the appearance of this new type of bound states is related to the presence of coupling between the neighboring lasers, and it is impossible in a solitary array element, where the zero intensity steady state is linearly unstable and pulse interaction is nonlocal and always repulsive. Furthermore, unlike the case of complex Ginzburg-Landau-type equations, the new bound pulse train regime can exhibit a continuously changing phase difference between the pulses depending on their time separation and correspond to a finite number of fixed points

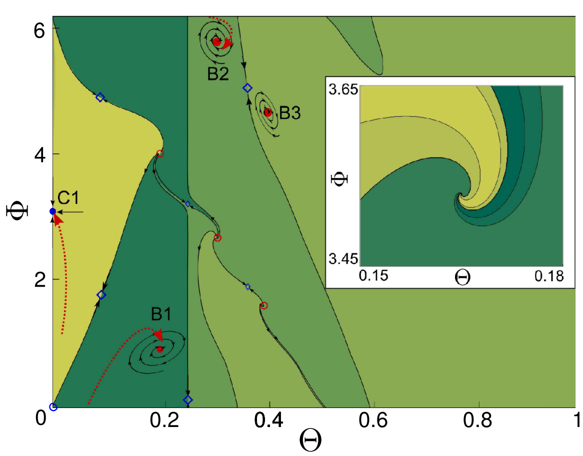

FIG. 4. Stable equilibria and their basins of attraction on the phase plane of the reduced system (7) for coupling phase $\varphi = 3.0$. **C1** corresponds to the stable antiphase synchronized solution. Equilibria **B1**, **B2**, and **B3** correspond to bound states with increasing time separation Θ, which have different phase shifts Φ between pulse intensity maxima. Inset: An example of the intertwining basins of attraction of five stable bound states in the vicinity of a unstable spiral source for Eq. (7) for $\varphi = 3.99$.

distributed nonequidistantly along the time axis. Since the physical mechanism of the bound state formation due to the coupling between neighboring lasers is quite general, it can be observed in other physical systems described by coupled sets of partial or delay differential equations, where pulse solutions are present. Therefore, we believe that our results are generic and valid for a large class of coupled spatially extended systems of different physical origin.

We thank the German Research Foundation (DFG) for financial support in the framework of the Collaborative Research Center 910, Project A3, and Collaborative Research Center 787, Project B5. A. V. also acknowledges the support of Grant No. 14-41-00044 of the Russian Scientific Foundation.

[1] N. N. Rosanov, *Spatial Hysteresis and Optical Patterns* (Springer, Berlin, 2002).
[2] H. Vahed, F. Prati, M. Turconi, S. Barland, and G. Tissoni, Phil. Trans. R. Soc. A **372** (2014).
[3] M. G. Clerc, A. Petrossian, and S. Residori, Phys. Rev. E **71**, 015205 (2005).
[4] F. Arecchi, S. Boccaletti, and P. Ramazza, Phys. Rep. **318**, 1 (1999).
[5] N. Akhmediev and A. Ankiewicz, in *Dissipative Solitons: From Optics to Biology and Medicine*, edited by N. Akhmediev and A. Ankiewicz, Lecture Notes in Physics Vol. 751 (Springer, Berlin, 2008).
[6] O. Lioubashevski, H. Arbell, and J. Fineberg, Phys. Rev. Lett. **76**, 3959 (1996).
[7] D. J. B. Lloyd, C. Gollwitzer, I. Rehberg, and R. Richter, J. Fluid Mech. **783**, 283 (2015).
[8] H. H. Rotermund, S. Jakubith, A. von Oertzen, and G. Ertl, Phys. Rev. Lett. **66**, 3083 (1991).
[9] A. S. Mikhailov and K. Showalter, Phys. Rep. **425**, 79 (2006).
[10] H.-G. Purwins, H. U. Bödeker, and S. Amiranashvili, Adv. Phys. **59**, 485 (2010).
[11] A. W. Liehr, *Dissipative Solitons in Reaction Diffusion Systems. Mechanism, Dynamics, Interaction* (Springer, Berlin, 2013).
[12] M. Suzuki, T. Ohta, M. Mimura, and H. Sakaguchi, Phys. Rev. E **52**, 3645 (1995).
[13] S. Barland, M. Giudici, G. Tissoni, J. R. Tredicce, M. Brambilla, L. Lugiato, F. Prati, S. Barbay, R. Kuszelewicz, T. Ackemann, W. J. Firth, and G.-L. Oppo, Nat. Photonics **6**, 204 (2012).
[14] P. Grelu and N. Akhmediev, Nat. Photonics **6**, 84 (2012).
[15] C. Elphick, E. Meron, J. Rinzel, and E. Spiegel, J. Theor. Biol. **146**, 249 (1990).
[16] J. N. Kutz, B. C. Collings, K. Bergman, and W. H. Knox, IEEE J. Quantum Electron. **34**, 1749 (1998).
[17] M. Nizette, D. Rachinskii, A. Vladimirov, and M. Wolfrum, Physica D (Amsterdam) **218**, 95 (2006).
[18] P. Camelin, J. Javaloyes, M. Marconi, and M. Giudici, Phys. Rev. A **94**, 063854 (2016).
[19] J. Javaloyes, M. Marconi, and M. Giudici, Phys. Rev. Lett. **119**, 033904 (2017).
[20] N. Akhmediev and A. Ankiewicz, *Solitons, Nonlinear Pulses and Beams* (Chapman and Hall, London, 1997).
[21] N. Akhmediev, A. Ankiewicz, and J. M. Soto-Crespo, J. Opt. Soc. Am. B **15**, 515 (1998).
[22] P. Grelu, F. Belhache, F. Gutty, and J.-M. Soto-Crespo, Opt. Lett. **27**, 966 (2002).
[23] D. Y. Tang, B. Zhao, D. Y. Shen, C. Lu, W. S. Man, and H. Y. Tam, Phys. Rev. A **66**, 033806 (2002).
[24] N. H. Seong and D. Y. Kim, Opt. Lett. **27**, 1321 (2002).
[25] L. M. Zhao, D. Y. Tang, X. Wu, D. J. Lei, and S. C. Wen, Opt. Lett. **32**, 3191 (2007).
[26] C. P. Schenk, P. Schütz, M. Bode, and H.-G. Purwins, Phys. Rev. E **57**, 6480 (1998).
[27] J. H. Lin, C. W. Chan, H. Y. Lee, and Y. H. Chen, IEEE Photonics J. **7**, 1 (2015).
[28] A. G. Vladimirov, G. V. Khodova, and N. N. Rosanov, Phys. Rev. E **63**, 056607 (2001).
[29] B. Ortać, A. Zaviyalov, C. K. Nielsen, O. Egorov, R. Iliew, J. Limpert, F. Lederer, and A. Tünnermann, Opt. Lett. **35**, 1578 (2010).
[30] X. Wu, D. Tang, X. Luan, and Q. Zhang, Opt. Commun. **284**, 3615 (2011).
[31] X. L. Li, S. M. Zhang, Y. C. Meng, Y. P. Hao, H. F. Li, J. Du, and Z. J. Yang, Laser Phys. **22**, 774 (2012).
[32] L. Gui, X. Xiao, and C. Yang, J. Opt. Soc. Am. B **30**, 158 (2013).
[33] V. Tsatourian, S. V. Sergeyev, C. Mou, A. Rozhin, V. Mikhailov, B. Rabin, P. S. Westbrook, and S. K. Turitsyn, Sci. Rep. **3**, 3154 (2013).
[34] G. Osipov, J. Kurths, and C. Zhou, *Synchronization in Oscillatory Networks*, Springer Series in Synergetics (Springer, Berlin, 2007).
[35] A. Pikovsky, M. Rosenblum, and J. Kurths, *Synchronization: A Universal Concept in Nonlinear Sciences*, Cambridge Nonlinear Science Series (Cambridge University Press, Cambridge, England, 2001).
[36] A. G. Vladimirov and D. Turaev, Phys. Rev. A **72**, 033808 (2005).
[37] P. J. Delfyett, S. Gee, M.-T. Choi, H. Izadpanah, W. Lee, S. Ozharar, F. Quinlan, and T. Yilmaz, J. Lightwave Technol. **24**, 2701 (2006).
[38] *Diode Laser Arrays*, edited by D. Botez and D. R. Scifres, Cambridge Studies in Modern Optics No. 14 (Cambridge University Press, Cambridge, England, 2008).
[39] S. A. Kashchenko, Comput. Math. Math. Phys. **38**, 443 (1998).
[40] G. Giacomelli and A. Politi, Phys. Rev. Lett. **76**, 2686 (1996).
[41] S. Yanchuk and G. Giacomelli, J. Phys. A **50**, 103001 (2017).
[42] M. Golubitsky, I. Stewart, and D. G. Schaeffer, *Singularities and Groups in Bifurcation Theory. Volume II*, Applied Mathematical Sciences Vol. 69 (Springer-Verlag, New York, 1988), p. 533.
[43] R.-d. Li and T. Erneux, Phys. Rev. A **46**, 4252 (1992).
[44] G. Kozyreff, A. G. Vladimirov, and P. Mandel, Phys. Rev. Lett. **85**, 3809 (2000).
[45] G. Kozyreff, A. G. Vladimirov, and P. Mandel, Phys. Rev. E **64**, 016613 (2001).
[46] S. Yanchuk and M. Wolfrum, Phys. Rev. E **77**, 026212 (2008).

[47] O. D'Huys, R. Vicente, T. Erneux, J. Danckaert, and I. Fischer, Chaos **18**, 037116 (2008).
[48] L. M. Pecora and T. L. Carroll, Phys. Rev. Lett. **80**, 2109 (1998).
[49] N. Rebrova, G. Huyet, D. Rachinskii, and A. G. Vladimirov, Phys. Rev. E **83**, 066202 (2011).
[50] R. Arkhipov, A. Pimenov, M. Radziunas, D. Rachinskii, A. G. Vladimirov, D. Arsenijević, H. Schmeckebier, and D. Bimberg, IEEE J. Sel. Top. Quantum Electron. **19**, 1100208 (2013).
[51] R. M. Arkhipov, T. Habruseva, A. Pimenov, M. Radziunas, S. P. Hegarty, G. Huyet, and A. G. Vladimirov, J. Opt. Soc. Am. B **33**, 351 (2016).
[52] See Supplemental Material at http://link.aps.org/supplemental/10.1103/PhysRevLett.119.163901 for the expanded expressions and coefficients used in this Letter, generalization to the case of N coupled lasers, and the video which shows the fixed points and their basins of attraction for the bound pulse trains in the system of two lasers for various coupling phases.
[53] S. Guo and J. Wu, *Bifurcation Theory of Functional Differential Equations*, Applied Mathematical Sciences (Springer, New York, 2013).
[54] D. Turaev, A. G. Vladimirov, and S. Zelik, Phys. Rev. E **75**, 045601 (2007).
[55] B. A. Malomed, Phys. Rev. A **44**, 6954 (1991).
[56] V. V. Afanasjev, B. A. Malomed, and P. L. Chu, Phys. Rev. E **56**, 6020 (1997).
[57] K. Engelborghs, T. Luzyanina, and D. Roose, ACM Trans. Math. Softw. **28**, 1 (2002).